Dynamic tensile fracture test of semi flexible epoxy asphalt concrete

Yebo Fang*

Department of Municipal Engineering and Equipment,
Shandong Urban Construction Vocational College,
Jinan 250103, China
Email: yebof@mls.sinanet.com
*Corresponding author

Yongbing Guan

Jinan Engineering Polytechnic,
Engineering Management College,
Jinan 250200, China
Email: 24596531@qq.com

Abstract: In order to overcome the problems of large error and high failure rate existing in the fracture test method of asphalt concrete materials, the dynamic tensile fracture test of semi flexible epoxy asphalt concrete materials was proposed. This method uses digital image technology (DIC) to measure the displacement of asphalt concrete crack propagation process, accurately capture the fracture process of asphalt concrete material crack tip, and use tensile test to evaluate the low temperature cracking performance of semi flexible pavement material. The experimental results show that when the loading wavelength is increased to 900 μs, the error of the maximum tensile stress calculation value is reduced to 7.5%. There is obvious size effect on the tensile strength of concrete. The safety risk assessment model has higher security guarantee. At the same time, the required capital investment is lower, and the test failure rate is always lower than 20%.

Keywords: semi flexible epoxy asphalt; concrete; digital image technology; DIC; tensile fracture.

Reference to this paper should be made as follows: Fang, Y. and Guan Y. (2021) 'Dynamic tensile fracture test of semi flexible epoxy asphalt concrete', *Int. J. Materials and Product Technology*, Vol. 63, Nos. 1/2, pp.33–47.

Biographical notes: Yebo Fang received his Master's in Construction and Civil Engineering from Shandong Construction University in 2014. Currently, he is an Associate Professor in the Department of Municipal Engineering and Equipment of Shandong Urban Construction Vocational College. His research interests include road and bridge engineering technology, municipal engineering technology, and road and bridge building materials.

Yongbing Guan received her Master's in Project Management from Tianjin University in 2008. Currently, she is an Associate Professor in the Engineering Management College of Jinan Engineering Polytechnic. Her research interests include project cost and construction project management.

1 Introduction

Under the background of rapid development of highway construction, the pressure of highway maintenance is gradually increasing. At present, the distance of highway maintenance in China has reached 4.6767 million kilometres, accounting for 97.9% of the total highway mileage (Wu et al., 2019). Therefore, it is necessary to invest huge resources to support, and due to the sustainability and long-term nature of highway maintenance construction, the consumption of resources in highway maintenance projects will increase. This not only has higher demand for maintenance technology and management, but also should be further developed and optimised in order to reduce the proportion of highway maintenance (Hwang et al., 2020). Semi flexible pavement is characterised by adding flexible materials into cement concrete mixture, to a certain extent, the anticracking performance of concrete is guaranteed, and the modulus is reduced. During the driving process, the comfort of the pavement is increased, and the service life of the pavement is increased. The new composite is formed by pouring the cement-based slurry with certain mechanical strength into the large gap base asphalt mixture The pavement structure can overcome the defects of traditional asphalt pavement, such as the weakening of anti-deformation ability and strength under high temperature environment, and the poor driving comfort and continuity of cement pavement, which is also overcome, and the pavement resistance to load is strengthened (Guo et al., 2020). Compared with ordinary asphalt pavement, high temperature stability, fatigue resistance and skid resistance are effectively improved. However, there are few researches on the cracking performance of semi permeable concrete pavement. In order to improve the application performance of asphalt concrete materials, it is necessary to study the tensile fracture performance of pavement to ensure the stability of pavement and improve the driving safety of pavement.

Le (2019) is to explore the mechanism of asphalt concrete pavement fatigue characteristics reduction under salt-rich freeze-thaw conditions. The asphalt concrete specimens of AC-20, AC-16 and AC-13 were prepared through indoor experiments, and the water accumulation of the road surface was analysed under the conditions of unspreading and sprinkling de-icing with clear water and saturated NaCl solution, respectively. Under the environment of 20°C to 50°C, the temperature change of the asphalt concrete pavement during use is simulated. The number of freeze-thaw cycles is controlled indoors to simulate the freeze-thaw action conditions of the actual road surface service process. Three stress ratios are selected. Asphalt mixture specimens were subjected to tensile fatigue test, and the influence of various conditions on the fatigue characteristics of multi-graded asphalt concrete was obtained. The research results provide reference value for guiding the design and construction of road surface and the spreading of deicing salt in winter. However, the research cost of this method is high, which severely limits the application scope of this method. Shao et al. (2020) indirect tensile test was performed on Marshall specimens on MTS testing machine, and the toughness index was used to analyse the influence of basalt fibre on asphalt concrete. The addition of fibres of different degrees can improve AC-13 and AC-20 asphalt. The deformation capacity, toughness index, failure load and horizontal deformation corresponding to the maximum load of the concrete before and after cracking, and the

toughness index reaches the maximum when the fibre content is 0.4%, the toughening effect is obvious, and the crack resistance is good in low temperature environment, but this method has big problems. Li et al. (2019) tensile test is carried out by MTS universal testing machine to obtain the force, displacement and time parameters during the test. At the same time, industrial CT equipment is used to scan the test pieces before and after the test to extract asphalt mortar, coarse aggregate and observe the crack propagation process of the specimen, and collect the load, displacement and the number of fractures between the unit particles during the simulation test. The characteristics of the load-displacement curve of the indoor test and the simulation test are compared and analysed. And based on Ncb, the internal damage degree Dm is proposed. Based on the overall crack image of the specimen, a box-counting dimension index Dc is proposed to analyse the relationship between damage and crack propagation, but the research accuracy of this method still needs to be further improved.

In order to solve the problems of high failure rate and high cost of the above methods, a new semi-flexible epoxy asphalt concrete material dynamic tensile fracture test method is proposed. The overall research plan of the method is as follows:

1 Introduce digital image related technology to accurately measure the displacement during the crack propagation process of asphalt concrete by calculating the connected void ratio and regional similarity.

2 According to the displacement measurement results, capture the fracture process of the crack tip of the asphalt concrete material, and conduct the concrete tensile fracture test through the universal machine.

3 Experimental verification. The proposed method is compared with three traditional methods based on the experimental comparison index of capital investment and failure rate.

Novelty: Here, we study the accurate measurement of crack propagation displacement using digital image correlation technology. Digital image-related technology is one of the optical mechanics methods. It is characterised by full-field non-contact measurement. It has low requirements for the experimental environment, uncomplicated experimental facilities, and has strong anti-interference ability. In the process of engineering material mechanics testing, has obvious advantages and is widely used in the deformation monitoring process of different structure types, and plays a more important role in the non-destructive testing process of structures.

2 Study on dynamic tensile fracture of semi flexible epoxy asphalt concrete

2.1 Crack propagation displacement measurement based on digital image

Compared with other asphalt concrete pavements, the composition of semi flexible pavement is more complex. In general, it is necessary to mix asphalt materials with cement slurry with high connectivity according to a certain proportion Wang et al. (2018). The structure of semi flexible pavement material is shown in Figure 1.

Figure 1 Composition of semi flexible pavement materials

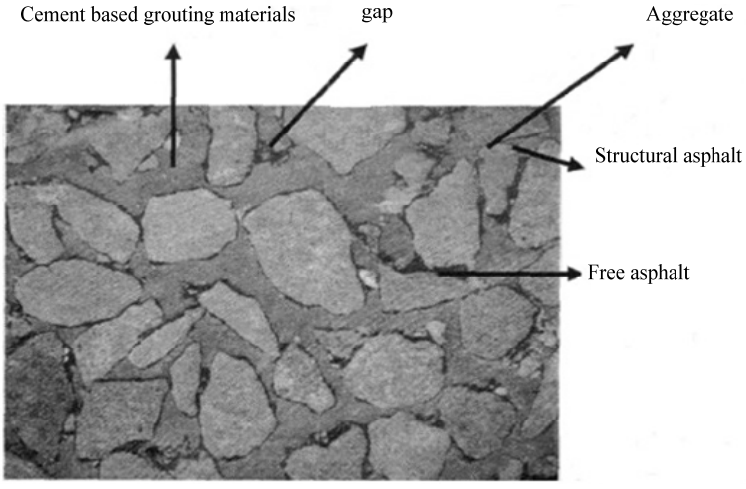

Uneven filling of asphalt mixture occurs from time to time. It is not only necessary to ensure the same void ratio of mixture, but also there is closed gap between asphalt mixture, which cannot be filled, which leads to uneven filling of cement mortar (Chen et al., 2018a). It is one of the effective methods to ensure the close filling between the mixtures to calculate the connected porosity of the mixture. The calculation method of the connected porosity is as follows:

$$VV_1 = \frac{V - V_1}{V} \times 100 \tag{1}$$

where V is the volume of the specimen, cm^3, V_1 is the volume of ore and closed hole, cm^3. There is a positive correlation between the connected voids and the voids between asphalt mixtures, which is unfavourable for slurry grouting, which will lead to excessive slurry injection, increase the rigidity of semi flexible pavement materials, and cannot meet the requirements of semi flexible pavement (Zhang, 2018). In order to ensure the performance of semi flexible pavement, the porosity is 30% and the connected porosity is 27%.

Before the tensile fracture deformation, assuming that the coordinates of a certain point on the speckle pattern are (x, y), and the coordinates are taken as the centre, a square area with the side length of N is selected. After the tensile deformation, an area of the same shape is obtained, and the side length is N. The maximum value of the prior coefficient of the two regions is supposed to correspond. The midpoint of the deformed area is expressed as (x', y'), and the pixel displacement in the region is calculated (Wang et al., 2019).

According to the standard covariance correlation function, the similarity degree of square area was calculated:

$$c = \frac{\sum\sum\left[\left(f - < f >\right) \cdot \left(g - < g >\right)\right]}{\left[\sum\sum\left(f - < f >\right)^2 \cdot \sum\sum\left(g - < g >\right)^2\right]^{\frac{1}{2}}} \tag{2}$$

In the formula, c ranges from Ganesh and Murthy (2019), with the highest similarity at $c = 1$ and the lowest at $c = 0$, and $f = f(x, y)$ and $g = g(x + u, y + v)$ represent the grey values of the speckle pattern centred on the source and target points, u, v represent the horizontal and vertical displacement, and $\langle f \rangle$, $\langle g \rangle$ represent the average grey value of the system.

Through the calculation results of regional similarity degree, the crack expansion displacement is calculated, which provides effective data for the dynamic tensile fracture test of materials.

2.2 Dynamic tensile fracture test

The cracking process of asphalt concrete at intermediate temperature is very complex. The development of cracks is accompanied by creep deformation and energy dissipation that cannot be ignored. Therefore, the energy criterion method is more suitable for the analysis of intermediate temperature cracking of asphalt concrete (Ganesh and Murthy, 2019).

Based on the measured results of crack propagation, the crack initiation and crack propagation of the model are reflected by the failure of the element. The element crack can be judged by the maximum stress damage criterion, and the propagation law of the crack is judged by the energy dissipation principle. The cracking process curve of asphalt concrete is shown in Figure 2.

Figure 2 Cracking process curve

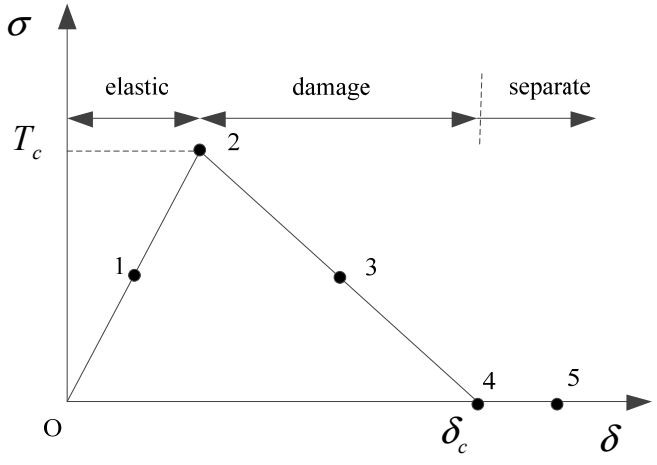

The damage model of asphalt concrete is continuous, and the evolution of failure surface is controlled by hardening variable ε^{pl}, the tensile characteristic strain can be judged by the following formula:

$$\sigma = (1-d)\, D_0^{el} : \left(\varepsilon - \varepsilon^{pl}\right) = D^{el} : \left(\varepsilon - \varepsilon^{pl}\right) \tag{3}$$

where d is the stiffness degradation variable with values between 0-1, '0' means no damage and '1' represents complete failure, D_0^{el} is the elastic stiffness of the concrete material without initial damage, D^{el} is the plastic strain tensor, and ε^{pl} is the elastic stiffness of the concrete material at strength d.

The tensile strength of concrete is relatively strong, which is more sensitive to the parameters such as elastic modulus and Poisson's ratio (Yu et al., 2018). The strength of concrete is analysed and expressed by the strength amplification factor dif corresponding to the strain rate. The tensile strength increase behaviour (TDIF) is expressed by the modified CEB model:

$$TDIF = \frac{f_{td}}{f_{ts}} = \beta\left(\frac{\dot{\varepsilon}_d}{\dot{\varepsilon}_{ts}}\right)^{1/3}, \dot{\varepsilon}_d > 1/s \tag{4}$$

where f_{td} is the dynamic tensile strength of concrete at a strain rate of $\dot{\varepsilon}_d$, f_{ts} is the static tensile strength, and β is the axial tensile strength of concrete under quasi-static conditions.

$\beta_{\dot{\varepsilon}}$ represents the influence relationship between strain rate and size effect, and the corresponding relationship between $\beta_{\dot{\varepsilon}}$ and $\lg(\dot{\varepsilon})$ can be represented by Figure 3.

Figure 3 Representation of influence coefficient (see online version for colours)

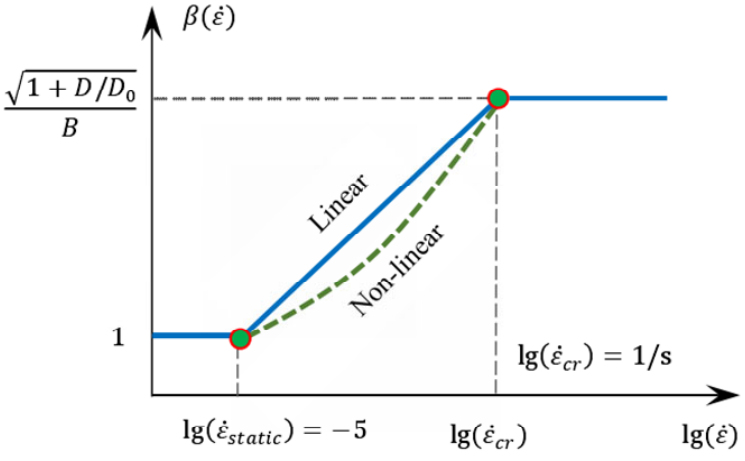

When the strain rate is $\dot{\varepsilon} \le 10^{-5}/s$, it is quasi-static, and the strain rate has no effect on the size effect, that is $\beta_{\dot{\varepsilon}} = 1$. When the strain rate is $\dot{\varepsilon} = 1/s$, the size effect is completely suppressed:

$$\sigma_{Nu}^{\dot{\varepsilon}} = f_t^{'} \cdot \varphi_{\dot{\varepsilon}} \tag{5}$$

where f_t is the static tensile strength of concrete and $\varphi_{\dot{\varepsilon}}$ is the enhancement effect coefficient of tensile strength.

The stress concentration will appear at the tip of asphalt material due to internal or external cracks or defects under load (Zhang et al., 2019). When the local stress exceeds the strength of the material, the crack or propagation rate of the material is too fast, and the average stress cannot meet the judgment of the fracture strength and failure characteristics of the asphalt material. Combined with the stress intensity factor *K*, the following cusp stress characteristics under load are expressed:

$$K = Y \cdot \sigma\sqrt{a} \tag{6}$$

where Y is the size factor, which is related to the shape of the crack and the geometry of the specimen, σ is the stress value, and a is the crack length. If the stress increases continuously, the stress intensity factor at the crack tip will reach the critical value. This state can be expressed as K_c, which can be called fracture toughness, which can be used to express the strength of preventing concrete from cracking (Alhussainy et al., 2019). The calculation method is as follows:

$$K_c = Y \cdot \sigma_c \sqrt{a_c} \tag{7}$$

where σ_c is the applied stress in the critical state and a_c is the crack length in the critical state.

During the fracture test, it is found that the crack surface will move before the crack propagation, and the original sharp crack tip will be passivated by plastic deformation. The passivation degree of the crack is directly proportional to the toughness of the material (Chen et al., 2018b). Therefore, CTOD, the opening displacement at the crack tip, is proposed as a criterion to measure the fracture toughness of the material. The displacement of the fracture tip can be calculated by measuring the CTOD. The schematic diagram of crack tip passivation and CTOD is shown in Figure 4.

Figure 4 Schematic diagram of crack tip passivation and CTOD

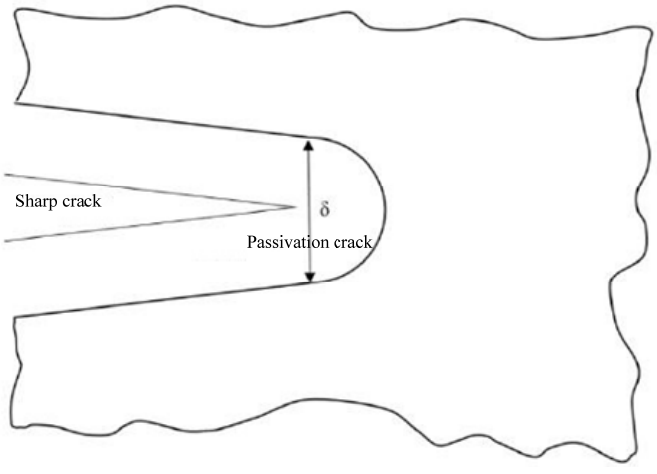

Assuming that the effective length at the back end of the crack tip is expressed as r_y, half of the width u_y of the crack tip after passivation can be expressed as follows:

$$u_y = \frac{\kappa + 1}{2\mu} K_1 \sqrt{\frac{r_y}{2\pi}} = \frac{4}{E'} K_1 \sqrt{\frac{r_y}{2\pi}} \tag{8}$$

$$r_y = \frac{1}{2\pi} \left(\frac{K_1}{\sigma_{YS}} \right) \tag{9}$$

where E' is the effective Young's modulus and σ_{YS} is the yield stress at the crack tip.

The fracture parameter CTOD is calculated as follows:

$$CTOD = \sigma = 2u_y = \frac{4}{\pi}\frac{K_I^2}{\sigma_{YS}E} \tag{10}$$

Due to the concentration of stress, crack discontinuity appears infinite singularity, which leads to infinite stress at the tip, and stress concentration will lead to material fracture. The relevant calculation diagram of cohesion is shown in Figure 5.

Figure 5 Schematic diagram of cohesion calculation

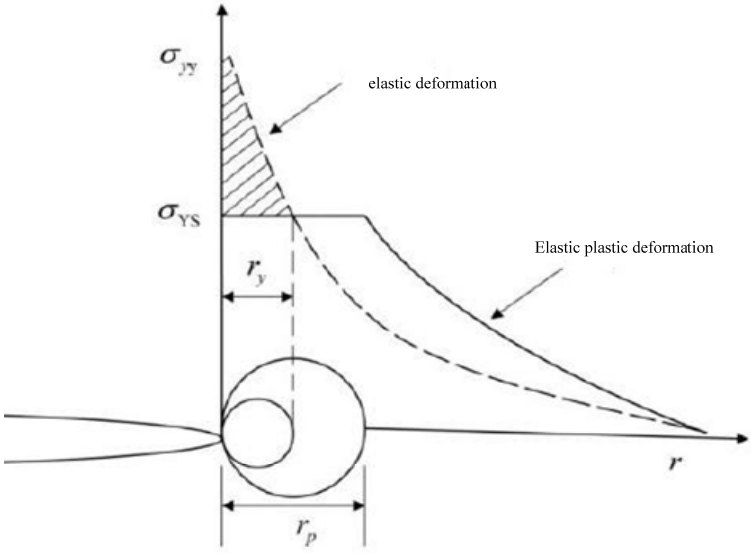

In order to ensure the stress balance, the stress of the specimen will change after the material is stretched. In order to ensure that the stress in the cohesive zone is less than the yield stress of the material, the cohesive zone diameter is r_p. The method is as follows:

$$\sigma_{YS}r_p = \int_0^{r_y} \sigma_{yy}dr = \int_0^{r_y} \frac{K_I}{\sqrt{2\pi r}}dr \tag{11}$$

$$r_p = \frac{1}{2\pi}\left(\frac{K_1}{\sigma_{YS}}\right)^2 \tag{12}$$

The constitutive relation between CTOD and fracture parameters under the condition of on-line elasticity and elastoplasticity is elaborated in detail by fracture mechanics theory.

In conclusion, digital image technology (DIC) is used to measure the displacement of asphalt concrete crack propagation process, accurately capture the fracture process of asphalt concrete material crack tip, and evaluate the performance of semi flexible pavement through tensile test.

3 Experimental study

3.1 Experimental data and indicators

In order to study the tensile fracture properties of semi flexible pavement, the universal machine test was carried out. The size of the trabecula is 260 mm × 40 mm × 50 mm, and eight specimens can be cut out from one rutting. Before the test, the specimens are placed in the freezing environment for more than 5 h, and the interval between the specimens during the freezing period shall not be less than 5 mm. The test equipment is MTS810 universal machine, and the finite element software ANSYS/LS-DYNA is used to simulate the experiment. The sample picture is shown in Figure 6.

Figure 6 Sample picture, (a) trabeculae (b) Marshall specimen (see online version for colours)

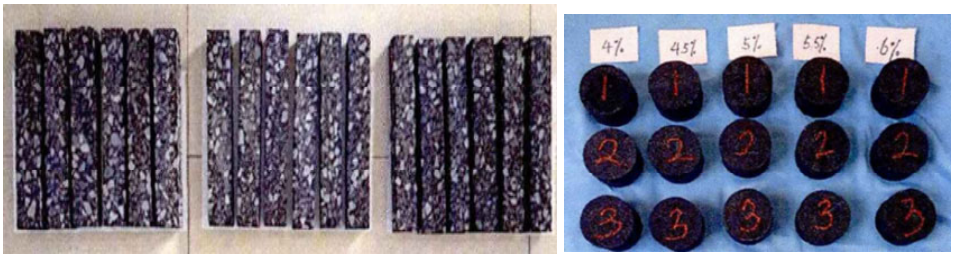

(a) (b)

In order to ensure the uniform temperature distribution in the specimen, the Marshall specimen was placed in the incubator with the temperature of –10°C for 24 h. The schematic diagram of indirect tensile test of asphalt mixture is shown in Figure 7.

Sensors are placed on both sides of Marshall specimen, and coupling agent is used for coupling treatment. In order to avoid noise interference, the limit value of data acquisition is set at about 40 dB. In the process of test, lead is cut first to ensure good coupling effect between sensor and specimen. The test variable selection results are shown in Table 1.

After processing the image of the test specimen from loading to failure, the whole field strain of the specimen can be calculated by correlation calculation, and then the strain nephogram of the specimen at a certain moment of loading is drawn as follows. The strain nephogram of the test process is shown in Figure 8.

Table 1 Test variable selection results

Experimental variables	*Horizontal selection*
Types of asphalt	PG64-22, PG76-22
Aggregate size	NMAS9.5 mm, NMAS25 mm
Test temperature	–10°C, 0°C
loading rate	0.03 mm/min, 1.00 mm/min

It can be seen from the above figure that after the crack starts on the right side of the pre cut, there is an irregular deformation area in the front edge of the crack tip, and the deformation area on the left side fails to develop into a crack at last. Therefore, the

mechanism of crack formation needs to be further studied. At the contact point of the loading contact on the top of the specimen, the plastic deformation occurs in the area under the load. The cohesive zone and its energy dissipation should be considered in the calculation of fracture energy. The failure diagram of dynamic SCB test specimen at different wavelengths is shown in Figure 9.

Figure 7 Indirect tensile test of asphalt mixture (see online version for colours)

Figure 8 Strain nephogram of test process (see online version for colours)

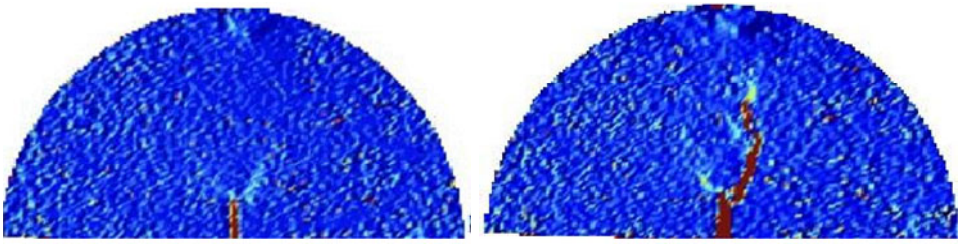

(a) (b)

Figure 9 Failure diagram of dynamic SCB test specimen at different wavelengths, (a) 100 μs (b) 300 μs (c) 900 μs

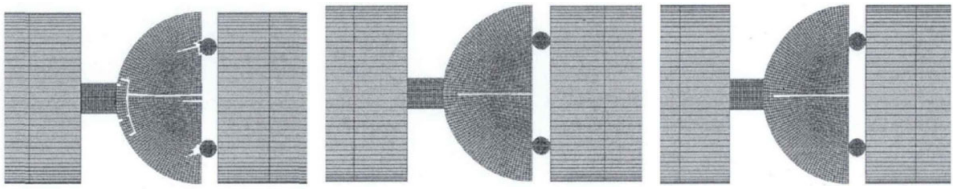

(a) (b) (c)

On the basis of the above environment, the overall experimental scheme is set as follows: maximum tensile stress calculation error, test safety level, failure rate as the experimental

comparison index, and the proposed method is compared with Le (2019), Shao et al. (2020) and Li et al. (2019).

1 The calculation error of maximum tensile stress is as follows:

The tensile state of the midpoint of the test change is unidirectional, and the maximum tensile stress at this point will be $\sigma_{t,\max}$, which can be calculated by the beam bending formula:

$$\sigma_{t,\max} = \frac{6FL}{hD^2} \tag{13}$$

where F is the loading force at the top of the specimen, L is the distance between the two loading supports on the straight side of the specimen, D is the diameter of the specimen, and h is the thickness of the specimen.

2 Test safety level: the safety level of evaluation model is the sum of the product of all evaluation index scores and their cumulative weights.

$$SV = \sum_{i=1} P_{C_i} W_{C_i} \tag{14}$$

where P_{C_i} is the score of the lowest evaluation index and W_{C_i} is the cumulative weight.

3 Failure rate: in the process of risk assessment, the failure rate will inevitably occur. The failure rate is calculated according to the time series method through the series formed by different test time data.

$$X_t = \sum_{i=1}^{p} \phi_i X_{t-i} + \varepsilon_i \tag{15}$$

where ϕ_i is the autoregressive coefficient, X_{t-i} is the zero mean fault rate time series, and ε_i is the white noise with independent distribution.

3.2 Calculation error of maximum tensile stress

The maximum tensile stress calculation value and error of dynamic SCB test sample under different wavelengths are shown in Table 2.

Table 2 Calculation value and error of maximum tensile stress of dynamic SCB test specimen under different wavelengths

Wavelength/μs	*Calculation value of maximum tensile stress/Mpa*	*Error value*
100	7.05	28.9%
300	9.47	8.1%
900	9.25	7.5%

It can be seen from the above results that during the tensile test, when the load reaches a certain value, there are many damages in the test. Under this state, the error of the maximum tensile stress value is large. When the loading force reaches 300 μs and 900 μs,

the failure position of the test starts directly at the midpoint, the failure results are the same, and the calculation error of the maximum tensile stress is small.

The relationship between the nominal stress (the ratio of the reaction force at the top of the specimen to the transverse area of the top of the specimen) and the nominal strain (the ratio of the vertical displacement of the top of the specimen to the height of the specimen) under different strain rates and sizes were simulated. The variation curve of tensile stress at different strain rates is shown in Figure 10.

Figure 10 Variation curve of tensile stress at different strain rates (see online version for colours)

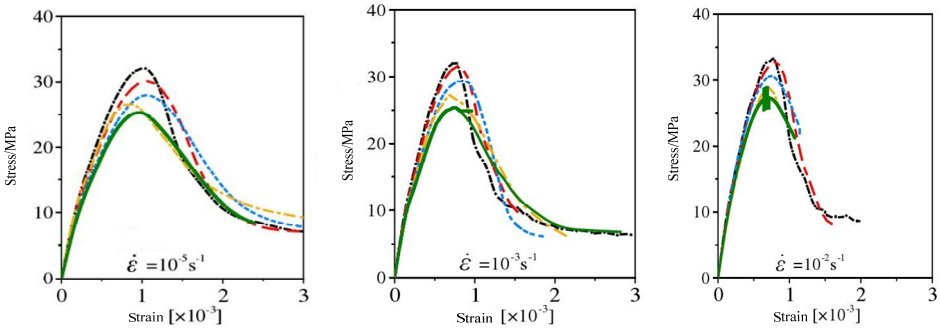

(a) (b) (c)

It can be seen from the above figure that the peak tensile stress (dynamic tensile strength) and corresponding peak tensile strain of concrete increase with the increase of strain stress. Under the same strain value, the value of stress peak value varies with the size of specimen, which indicates that the tensile strength of concrete specimen has obvious size effect under dynamic loading.

3.3 Comparison of test safety level

The safety level of the test safety risk assessment model is reflected in personnel quality investment, personnel training investment, construction technology level investment, construction equipment investment and operation platform investment, in which technology and equipment investment occupy the main position. With the increase of investment, the security risks in different aspects will be reduced. Under the condition of controlling the same investment, the security level of the traditional test security risk assessment model and the test security risk assessment model in this paper are compared. The relationship between capital investment and safety level is shown in Figure 11.

As can be seen in Figure 11, with the increase of test fund investment, the overall test safety level shows an upward trend, but the test fund investment and the safety level cannot form a linear relationship. Compared with the traditional test security risk assessment model, the security level of the test security risk assessment model in this paper is significantly higher than that of the traditional method. Under the same security level, the investment of the test security risk assessment model in this paper is significantly lower than that of the traditional method. Therefore, it can be seen from Figure 11 that the test security risk assessment model designed in this paper has higher security guarantee and lower capital investment.

Figure 11 Relationship between test fund investment and safety level

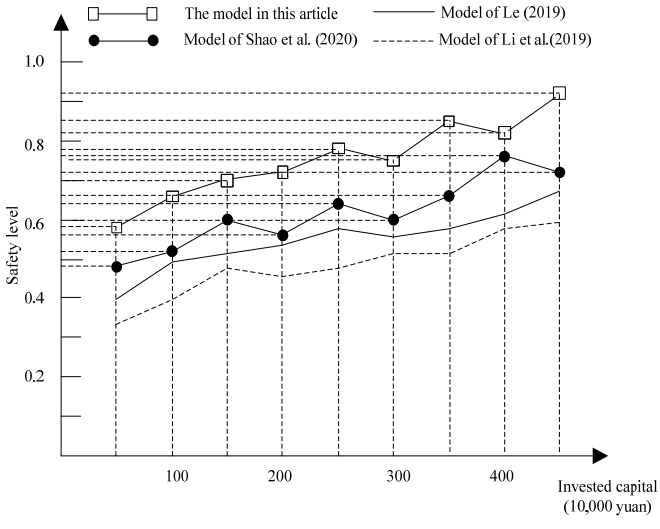

3.4 Failure rate comparison

The test failure rate is studied, and the test failure rate is compared with the traditional method through the statistics of the results. The failure rate comparison results are shown in Figure 12.

Figure 12 Test failure rate comparison results

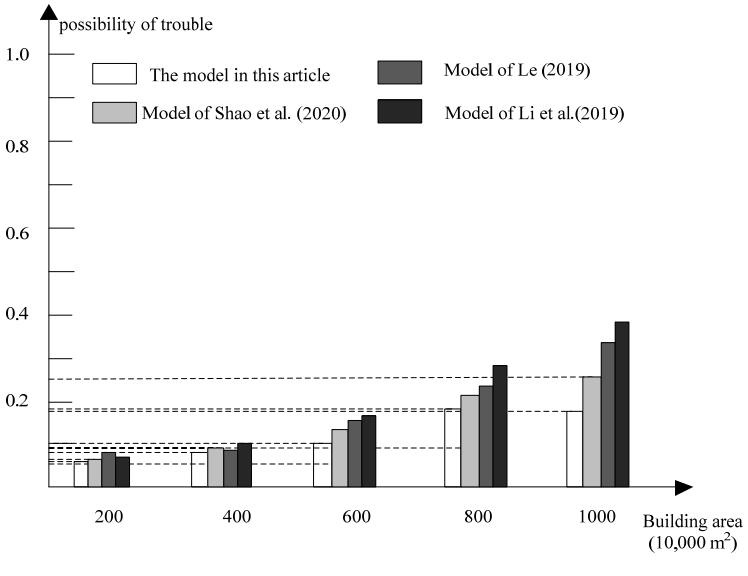

It can be seen from Figure 12 that the failure rate of the traditional method is always lower than 30%, while that of the method in this paper is always lower than 20%. Therefore, the test precision of this paper is higher than that of the traditional method,

and the service life is increased. In other words, the test performance of this paper is better than that of the traditional method. The main reason is that this method uses DIC to measure the displacement in the process of asphalt concrete crack propagation, accurately capture the fracture process of asphalt concrete material crack tip, and reduce the failure rate.

4 Conclusions

In order to improve the application safety of asphalt concrete, the dynamic tensile fracture test method of semi flexible epoxy asphalt concrete was proposed. It is proved that the method has lower error and cost in dynamic tensile fracture test of semi flexible epoxy asphalt concrete. When the loading wavelength is increased to 900 μs, the error of the calculated maximum tensile stress is reduced to 7.5%. There is obvious size effect on the tensile strength of concrete. The safety risk assessment model for testing has higher security guarantee. At the same time, the required capital investment is lower, and the test failure rate is always below 20%. However, due to the complexity of concrete under dynamic load, the structure and mechanism of asphalt concrete materials need to be further studied in high strain rate state.

Acknowledgements

This work was supported by Department of Vocational and Adult Education, Ministry of Education, China under grant no. 2019-63[2019]100.

References

Alhussainy, F., Hasan, H.A., Sheikh, M.N. and Hadi, M.S. (2019) 'A new method for direct tensile testing of concrete', *Journal of Testing & Evaluation*, Vol. 47, No. 2, pp.704–718.

Chen, X., Xu, L. and Bu, J. (2018) 'Dynamic tensile test of fly ash concrete under alternating tensile-compressive loading', *Materials & Structures*, Vol. 51, No. 1, pp.20–26.

Chen, X., Xu, L. and Bu, J. (2018) 'Dynamic tensile test of fly ash concrete under alternating tensile-compressive loading', *Materials and structures*, Vol. 51, No. 1, pp.201–212.

Ganesh, P. and Murthy, A.R. (2019) 'Tensile behaviour and durability aspects of sustainable ultra-high performance concrete incorporated with GGBS as cementitious material', *Construction and Building Materials*, Vol. 19, No. 10, pp.667–680.

Guo, R.Q., Ren, H.Q., Zhang, L., Long, Z.L., Jiang, X.Q., Wu, X.Y. and Wang, H.L. (2020) 'Direct dynamic tensile study of concrete materials based on mesoscale model', *International Journal of Impact Engineering*, Vol. 40, No .9, pp.18–31.

Hwang, Y.K., Bolander, J.E. and Lim, Y.M. (2020) 'Evaluation of dynamic tensile strength of concrete using lattice-based simulations of spalling tests', *International Journal of Fracture*, Vol. 21, No. 2, pp.191–209.

Le, Q.L. (2019) 'Fatigue behavior of multi-stage asphalt concrete under salt rich freeze-thaw condition', *Aging and application of synthetic materials*, Vol. 48, No. 6, pp.83–88.

Li, X.L., Liu, X.Y., Lv, X.C. and Ye, J.H. (2019) 'Indirect tensile test of asphalt mixture based on discrete element method and fractal dimension', *Journal of Chang'an University (NATURAL SCIENCE EDITION)*, Vol. 39, No. 6, pp.39-48.

Shao, X.S., Li, C. and Pei, K. (2020) 'Analysis of crack resistance of basalt fiber asphalt concrete based on toughness index', *Journal of Inner Mongolia University of Technology (NATURAL SCIENCE EDITION)*, Vol. 39, No. 1, pp.70–76.

Wang, C., Yang, S., Li, X., Jiang, C.L. and Li, M.K. (2019) 'Study on the failure characteristics of concrete specimen under confining pressure', *Arabian Journal for Science and Engineering*, Vol. 44, No. 5, pp.4119–4129.

Wang, Y., Shijie, C., Lu, G.E., Zhou, L. and Hu, H.X. (2018) 'Analysis of dynamic tensile process of fiber reinforced concrete by acoustic emission technique', *Journal of Wuhan University of Technology (Materials Science Edition)*, Vol. 33, No. 5, pp.119–129.

Wu Z., Cui, W., Fan, L. and Liu, Q.S. (2019) 'Mesomechanism of the dynamic tensile fracture and fragmentation behaviour of concrete with heterogeneous mesostructure', *Construction and Building Materials*, Vol. 30, No. 17, pp.573–591.

Yu, J.H., Kishimoto, H., Nakazato, N. and Park, J.S. (2018) 'Specimen size effects on fracture behaviour of SiC/SiC tubes during circumferential tensile test', *Advanced Composite Materials*, Vol. 27, No. 5, pp.531–539.

Zhang, M., Qian, Z. and Huang, Q. (2019) 'Test and evaluation for effects of freeze-thaw cycles on fracture performance of epoxy asphalt concrete composite structure', *Journal of testing and evaluation*, Vol. 47, No. 1, pp.556–572.

Zhang, X. (2018) 'Simulation of bending fracture test process for asphalt concrete beam based on heterogeneous state', *Construction and Building Materials*, Vol. 36, No. 30, pp.10–18.